

Articles

Anionic Polymerization of (Meth)acrylates in the Presence of Cesium Halide–Trialkylaluminum Complexes in Toluene

Bardo Schmitt, Wolfgang Stauf, and Axel H. E. Müller^{*,†}

Universität Mainz, Institut für Physikalische Chemie, Wolderweg 15, D-55099 Mainz, Germany

Received October 1, 1999

ABSTRACT: The polymerization of methyl methacrylate and various acrylates initiated by ester enolates in the presence of cesium halide–trialkylaluminum complexes, $\text{Cs}[\text{Al}_n\text{R}'_{3n}\text{X}]$ ($n = 1, 2$; $\text{R}' = \text{Et}, \text{Bu}'$), in toluene has living and controlled character at -20°C for methacrylates ($\text{X} = \text{Cl}$) and at -65°C for *n*-butyl acrylate ($\text{X} = \text{F}$). Quantitative monomer conversions are usually reached, leading to polymers with narrow molecular weight distributions ($M_w/M_n < 1.1$). Kinetic investigations indicate a rather complex polymerization mechanism, and we assume an equilibrium between at least two active species. With this new initiating system, beside acrylate homopolymers, random and graft copolymers can be synthesized.

Introduction

In recent publications,^{1–4} we described the anionic polymerization of (meth)acrylates in the presence of tetraalkylammonium–trialkylaluminum 1:2 complexes, $\text{NR}_4[\text{Al}_2\text{R}'_6\text{X}]$, in toluene. The polymerization has living and controlled character at low temperatures for methyl methacrylate up to 0°C . Quantitative monomer conversions are usually reached within a few minutes, and the resulting polymers have narrow molecular weight distributions. Kinetic investigations show that the polymerization of MMA follows first-order kinetics with respect to initial concentrations of active centers, monomer, and $\text{NR}_4[\text{Al}_2\text{R}'_6\text{X}]$. At low concentrations of the complex the first-order time–conversion plots are curved, and the polymers are initially bimodal.³ The mechanism of the reaction is rather complex, implying equilibria between at least two active species of different reactivity.

Multinuclear NMR and quantum-chemical investigations on model compounds (ester enolates) enlightened the structure of active species in methacrylate polymerization in the presence of aluminum alkyl/tetraalkylammonium halide complexes in nonpolar solvents.⁵ It appears that the reaction of ethyl α -lithioisobutyrate (EiBLi) with these complexes in equimolar amounts leads to the slow formation of complexes $\text{NMe}_4[\text{EiBLi} \cdot \text{AlEt}_3\text{Cl}]$ and $\text{NMe}_4[\text{EiBLi} \cdot \text{AlEt}_3\text{Cl} \cdot \text{AlEt}_3]$. These species tend to associate due to an electron deficiency in the coordination sphere of lithium.

In the polymerization of primary acrylates it was found that only the complex of triisobutylaluminum and tetramethylammonium chloride enables a controlled polymerization at low temperatures (-78°C).^{1,6} At higher temperatures, termination reactions (backbiting) are observed. Again, the polymerization of *n*-butyl

acrylate (*n*BuA) follows first-order kinetics with respect to initial concentrations, but the mechanism of the polymerization appears to be rather complex.

Bandermann et al.⁷ observed Hofmann elimination or methylation ($\text{R} = \text{Me}$) in the metal-free anionic polymerization of MMA with tetrabutylammonium malonates in THF. Such side reactions have to be taken into account in our systems as well. Another problem arises from the rather high polymerization rates observed when synthesizing PMMA with low molecular weight. Then, rather high initiator concentrations are needed, leading to short reaction times ($t_{1/2} < 1$ min). The alkylammonium halide system can hardly be controlled since that would ask for mixing times of a few seconds—this cannot be achieved in a conventional stirred tank reactor. The high monomer concentrations needed in industrial processes would cause undesired exotherms of more than 10 K in fast polymerizations, thus enhancing the possibility of side reactions.

In the anionic polymerization of methyl methacrylate with EiBLi in the presence of ammonium alkyl halide–aluminum alkyl complexes in toluene at -20°C , it was found that the rate of polymerization decreases with decreasing size of the ammonium counterion.¹ The results suggested that a cation smaller than NMe_4^+ would lead to an even lower rate of polymerization. According to Ziegler et al.,⁸ not only tetraalkylammonium halides but also several alkali halides give soluble complexes ($\text{Me}[\text{Al}_n\text{R}'_{3n}\text{X}]$, $n = 1, 2$) with aluminum alkyls in toluene. This is our new concept in order to prevent the mentioned side reactions and achieve better reaction control. Thus, in the present work we wish to report on the effect of cesium halides in complexes with aluminum alkyls on the anionic polymerization of (meth)acrylates in toluene.

Experimental Part

Reagents. Ethyl α -lithioisobutyrate (EiBLi) was prepared according to the method of Lochmann and Lím.⁹ *tert*-Butyl-

[†] New address: Universität Bayreuth, Makromolekulare Chemie II, D-95440 Bayreuth, Germany. E-mail: axel.mueller@uni-bayreuth.de.

Table 1. Anionic Polymerization of MMA Initiated by EiBLi in the Presence of Various Salt/Triethylaluminum Complexes in Toluene at $-20\text{ }^{\circ}\text{C}^a$

salt	Al:(Cs/NR ₄):Li	[MMA] ₀ /mol L ⁻¹	[EiBLi] ₀ /10 ⁻³ mol L ⁻¹	$k_{\text{app}}/10^{-3}$ s ⁻¹	x_p	M_n	M_w/M_n	f	$[P^*]_0/10^{-3}$ mol L ⁻¹	$k_p/\text{mol L}^{-1} \text{ s}^{-1}$
CsCl	14:7:1	0.14	0.69	0.41	1.00	24 300	1.11	0.82	0.57	5.14
NBu ₄ Br	30:10:1	0.14	0.69	8.4	1.00	30 300	1.07	0.66	0.46	130
NOc ₄ Br	30:10:1	0.14	0.69	6.0	1.00	39 800	1.05	0.50	0.35	122
NBu ₄ Br	3:2:1	0.34	1.71	16.1	1.00	26 000	1.06	0.77	1.32	35.9
NMe ₄ Cl	3:1:1	0.72	3.44	4.8	1.00	30 000	1.12	0.67	2.30	2.9
CsCl	4:2:1	0.68	3.44	2.05	1.00	25 000	1.10	0.80	2.75	1.1

^a k_{app} = apparent rate constant, x_p = monomer conversion, f = initiator efficiency, $[P^*]_0$ = concentration of active species, k_p = rate constant of polymerization.

lithium (tBuLi) was purchased as 1.7 M solution in pentane (Aldrich), titrated, and used without further purification. Triethylaluminum (AlEt₃) and triisobutylaluminum (AlBu₃) were purchased as 25 wt % solutions in toluene (Aldrich) and used as received. Cesium fluoride and cesium chloride (Aldrich) were mixed with benzene and freeze-dried. *n*-Butyl acrylate (nBuA) and methyl methacrylate (MMA, both BASF AG) were fractionated from CaH₂ over a 1 m column filled with Sulzer packing at 45 mbar, stirred over CaH₂, degassed, and distilled in high vacuum. Toluene (BASF AG) was fractionated over a 1.5 m column, stirred twice over sodium/potassium alloy, degassed, and distilled in high vacuum. 2-Ethylhexyl acrylate (EHA), allyl acrylate (AlA), and dihydrodicyclopentadienyl acrylate (DCPA) (all BASF AG) were stirred over CaH₂, degassed, and filtrated over a short alumina column. Octane, decane, and tetradecane (internal standards for GC, Aldrich) were stirred over sodium/potassium alloy, degassed, and distilled in high vacuum.

Kinetics. All experiments were carried out in a stirred tank reactor under a nitrogen atmosphere. First, the cesium halide–aluminum alkyl complex was stirred for 5 min in toluene at the later polymerization temperature. After adding the initiator, the solution was stirred for further 5 min, and then the monomer was added. The polymerization was quenched with methanol/acetic acid (9:1 v/v), and monomer conversion was determined by GC using an alkane as internal standard. After evaporation of the solvent, the polymer was dissolved in benzene, filtered, and freeze-dried.

GPC. GPC was performed using THF as eluent at a flow rate of 1 mL/min. Detectors: 2 × JASCO-UVIDEC 100 III with variable wavelength and Bischoff RI detector 8110; column set: 2 × 60 cm, 5 μ PSS SDV gel, 100 Å; and linear: 10²–10⁵ Å. PMMA standards (PSS, Mainz) and PnBuA standards, which had been synthesized in our laboratory and characterized by MALDI-TOF MS and GPC/MALLS measurements, were used for calibration.

MALDI-TOF MS. Spectra were recorded with a Bruker Reflex mass spectrometer equipped with a nitrogen laser source delivering 3 ns pulses at $\lambda = 337$ nm. 1,8,9-Trihydroxyanthracene was used as matrix and potassium trifluoroacetate as cationization agent.

Results and Discussion

Polymerization of MMA. We first examined the effect of cesium chloride–aluminum alkyl complexes on the anionic polymerization of MMA with EiBLi in toluene at $-20\text{ }^{\circ}\text{C}$. The reaction usually follows first-order kinetics (Figure 1), and the number-average degree of polymerization increases linearly with monomer conversion (Figure 2). The polymers obtained have narrow molecular weight distributions and are free of cyclic β -ketoesters as indicated by the absence of a β -ketoester UV absorption in GPC ($\lambda = 300$ nm). All these findings suggest both living and controlled character of the polymerization. The time–conversion plots together with the data in Table 1 clearly show that the polymerization rate decreases when changing from alkylammonium halides to cesium halides—this confirms the suggestions given in the Introduction.

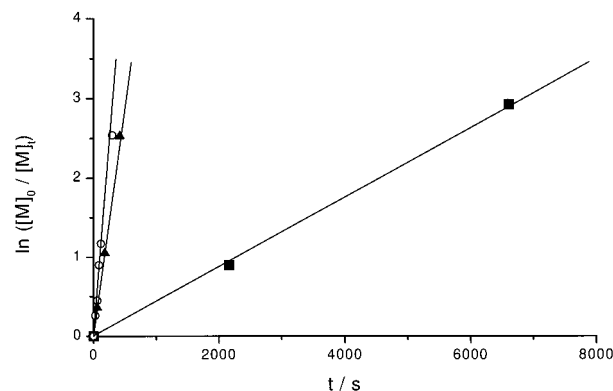


Figure 1. First-order time–conversion plots for the anionic polymerization of MMA initiated by EiBLi in toluene at $-20\text{ }^{\circ}\text{C}$ with Cs[Al₂Et₆Cl] (■), NBu₄[Al₂Et₆Br] (○), and NOc₄[Al₂Et₆Br] (▲). For reaction conditions see Table 1, entries 1–3.

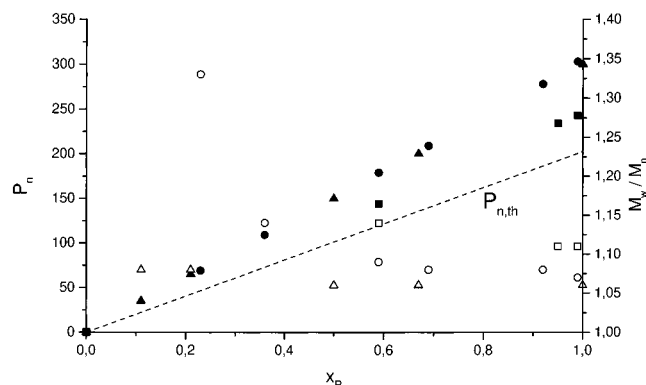


Figure 2. Plot of number-average degree of polymerization, P_n (■, ●, ▲), and polydispersity index, M_w/M_n (□, ○, △), vs monomer conversion, x_p , for the polymerization described in Figure 1.

Upon increasing the initiator concentration and thus decreasing the complex/initiator ratio, the time–conversion plots showed in some cases an upward curvature as has been observed with ammonium salts.³ Nonetheless, a linear plot of the number-average degree of polymerization vs monomer conversion is achieved in any case.

Block Copolymers PMMA-*b*-PtBuMA. The system described above can also be used to prepare block copolymers. As can be seen in Figure 3, the blocking efficiency from living PMMA to *tert*-butyl methacrylate (tBuMA) is improved from $f = 0.75$ for the NBu₄[AlEt₃Br] system to $f = 0.95$ for the Cs[AlEt₃Cl] system.

Other combinations of methacrylate monomers and cesium halides, e.g., polymerization of MMA with CsF or of tBuMA with CsCl, did not lead to polymerization at all.

Polymerization of *n*-Butyl Acrylate. Further, we studied the effect of cesium halide–aluminum alkyl

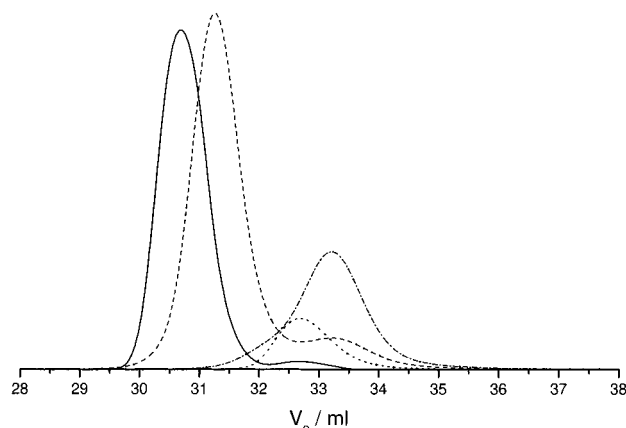


Figure 3. GPC eluograms of the block copolymers obtained from the anionic polymerization of MMA and tBuMA at -20°C in toluene with (a) $\text{EtBLi/NBu}_4[\text{AlEt}_3\text{Br}]$ and (b) $\text{EtBLi/Cs}[\text{AlEt}_3\text{Cl}]$. (a) Precursor PMMA (---), $M_n = 6600$, $M_w/M_n = 1.10$; block copolymer PMMA-*b*-PtBuMA (- - -), $M_n = 22\,200$, $M_w/M_n = 1.27$. (b) Precursor PMMA (\cdots), $M_n = 6800$, $M_w/M_n = 1.12$; block copolymer PMMA-*b*-PtBuMA (—), $M_n = 37\,600$, $M_w/M_n = 1.06$.

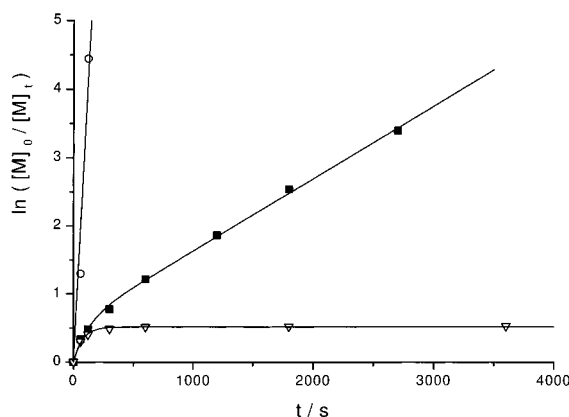


Figure 4. First-order time-conversion plots for the anionic polymerization of *n*BuA at -78°C with $\text{EtBLi/Cs}[\text{Al}_2\text{Bu}_6\text{X}]$ in toluene. CsCl (∇), CsF (\circ), Me_4NCl (\blacksquare). For reaction conditions see Table 2, entries 3–5.

complexes on the anionic polymerization of *n*-butyl acrylate with EtBLi in toluene at -78°C . In the presence of CsCl we only obtained a strongly curved time-conversion plot and incomplete monomer conversion, indicating the occurrence of termination reactions (Figure 4). The initial rate of polymerization is comparable to that observed with NMe_4Cl . Using CsF , time-conversion plots are linear and rates are much higher. The living character of the reaction is also indicated by a linear increase of the number-average degree of polymerization vs monomer conversion (see Figure 6) and by polymers with very narrow molecular weight distribution ($M_w/M_n \leq 1.1$, see Table 2). Compared to the polymerization system containing tetramethylammonium chloride,^{1,4} we have found reaction conditions to gain better reaction control.

In further experiments we investigated the effect of two different complexes, $\text{Cs}[\text{Al}_n\text{R}'_{3n}\text{F}]$ ($n = 1, 2$). In the polymerization in the presence of a 1:1 complex a linear first-order time-conversion plot was observed, whereas with a 1:2 complex the rate of polymerization increases during the course of reaction (Figure 5). Since linear plots of the number-average degree of polymerization vs monomer conversion are obtained (Figure 6), this observation can hardly be explained by a slow initiation

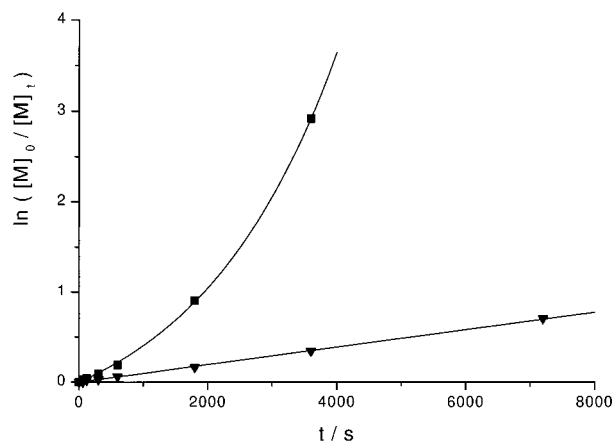


Figure 5. First-order time-conversion plots for the anionic polymerization of *n*BuA at -78°C with $\text{EtBLi/Cs}[\text{Al}_n\text{Bu}'_{3n}\text{F}]$ in toluene. $n = 1$: (∇); $n = 2$: (\blacksquare). For reaction conditions see Table 2, entries 1 and 2.

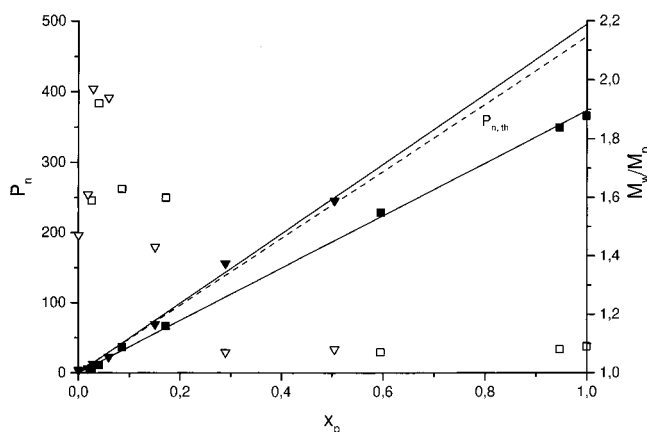


Figure 6. Plot of number-average degree of polymerization, P_n (\blacksquare , ∇), and polydispersity index, M_w/M_n (\square , ∇), vs monomer conversion, x_p , for the polymerization described in Figure 5; (---) theoretical P_n .

process. Thus, we assume that this is due to an equilibrium between active species of different reactivities.³ The resulting polymers display narrow molecular weight distributions ($M_w/M_n < 1.1$). Referring to GPC analysis with UV detection at $\lambda = 260\text{ nm}$,¹⁰ they are nearly free of cyclic β -ketoester end groups. All these results suggest that the polymerization lacks termination via backbiting and transfer reactions; i.e., it has living and controlled character. Surprisingly, the initiator efficiency, $f = P_{n,\text{th}}/P_{n,\text{exp}}$, in the polymerization with the 1:2 complex is higher than 100% (see Table 2); this will be discussed below.

Further experiments using $\text{Cs}[\text{Al}_2\text{Bu}'_6\text{F}]$ at different initial concentrations of EtBLi always gave such typical curved first-order time-conversion plots. The initial and the final slopes of the curved time-conversion plots correspond to apparent rate constants of propagation, k_{app} and k'_{app} , respectively (see Table 2). Regarding either rate constant, the reaction is first-order with respect to the concentration of the active centers, $[P^*]_0 = f[\text{EtBLi}]_0$ (Figure 7). The reaction also follows first-order kinetics for the initial concentration of monomer.⁶

Effect of the Complex Concentration. The first-order time-conversion plots are only linear for very low or very high concentrations of $\text{Cs}[\text{Al}_2\text{Bu}'_6\text{F}]$ (Figure 8). Otherwise, the slopes increase constantly during the polymerization. For both the initial and final apparent

Table 2. Anionic Polymerization of n BuA with $\text{EiBLi/Cs}[\text{Al}_n\text{Bu}_{3n}\text{X}]$ ($n = 1, 2$) in Toluene at -78°C^a

salt	Al:Cs:Li	$k_{\text{app}}/10^{-4}$ s^{-1}	$k'_{\text{app}}/10^{-4}$ s^{-1}	x_p^b	M_n	M_w/M_n	f	$[\text{P}^*]_0/10^{-4}$ mol L^{-1}	$k_p/$ $\text{mol L}^{-1} \text{s}^{-1}$	$k'_p/$ $\text{mol L}^{-1} \text{s}^{-1}$
CsF	3.6:3.5:1	1.0		0.51	31 600	1.08	0.99	4.5	0.22	
CsF	7.1:3.5:1	1.5	25.9	1.00	47 000	1.09	1.28	6.3	0.24	4.1
CsF	28.6:14.2:1	34.0		1.00	20 300	1.1	3.03	14.9	22.8	
CsCl	28.6:14.2:1	6.9		0.42	18 200	1.7	1.58	7.8	8.9	
NMe ₄ Cl	28.6:14.2:1	5.8	1.1	0.97	30 500	1.1	1.57	7.7	7.5	0.14

^a $[\text{EiBLi}]_0 = 4.9 \times 10^{-4} \text{ mol/L}$, $[n\text{BuA}]_0 = 0.234 \text{ mol/L}$. k_{app} , k'_{app} = initial and final apparent rate constants, respectively. ^b Conversion reached at longest reaction time.

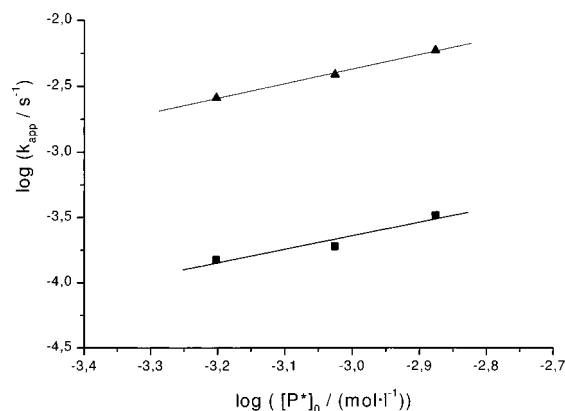


Figure 7. Determination of the reaction order with respect to the concentration of active centers, $[\text{P}^*]_0$, for the anionic polymerization of n BuA with $\text{EiBLi/Cs}[\text{Al}_2\text{Bu}_6\text{F}]$ in toluene at -78°C . $[n\text{BuA}]_0 = 0.234 \text{ mol/L}$, $[\text{AlBu}_3]/[\text{CsF}] = 3.5 \times 10^{-3} \text{ mol/L}$, $[\text{CsF}] = 1.7 \times 10^{-3} \text{ mol/L}$. Initial apparent rate constant (■), slope 1.0 ± 0.3 ; final apparent rate constant (▲), slope 1.1 ± 0.1 .

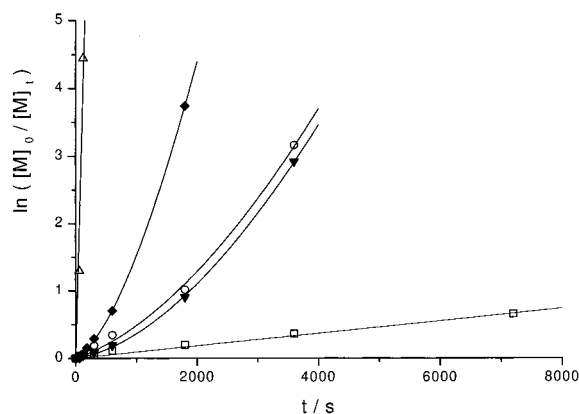


Figure 8. First-order time-conversion plots for the anionic polymerization of n BuA in toluene at -78°C with $\text{EiBLi/Cs}[\text{Al}_2\text{Bu}_6\text{F}]$ for different complex concentrations. $[\text{EiBLi}]_0 = 4.9 \times 10^{-4} \text{ mol/L}$, $[n\text{BuA}]_0 = 0.234 \text{ mol/L}$, $[\text{AlBu}_3]/[\text{CsF}] = (1.8/0.9)$ (□), $(3.5/1.7)$ (▼), $(5.3/2.6)$ (○), $(7.0/3.4)$ (◆), $(14.0/7.2)$ (△), all in 10^{-3} mol/L .

rate constants the polymerization is first-order with respect to the concentration of $\text{Cs}[\text{Al}_2\text{Bu}_6\text{F}]$ (Figure 9). Again, the plots of the number-average degree of polymerization with monomer conversion are linear; i.e., a slow initiation process can be excluded. The molecular weight distributions of the polymers are bimodal at low conversions but unimodal and narrow for higher monomer conversions.

Therefore, we assume a slow-reversible or irreversible-isomerization between at least two active species of different reactivity. This is in agreement with the studies on the polymerization in the presence of tetraalkylammonium/aluminum alkyl complexes, where similar structures of the active chain ends are dis-

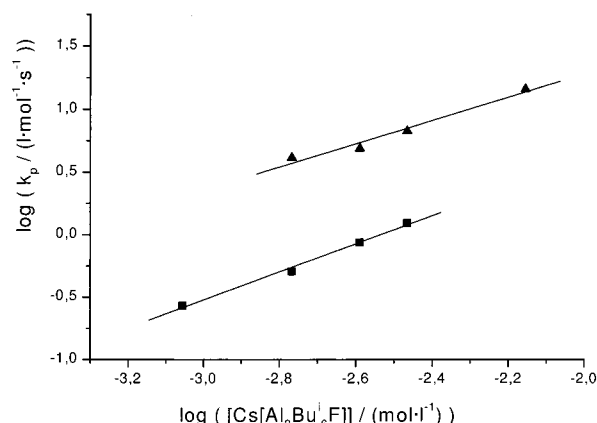
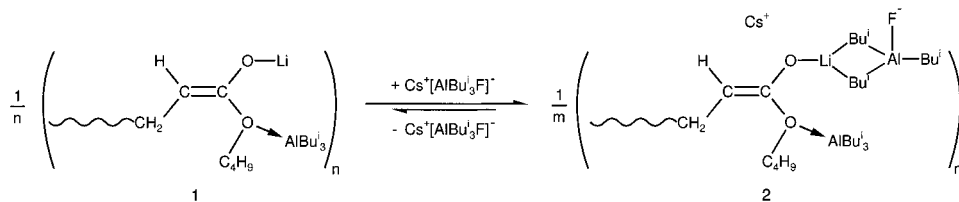
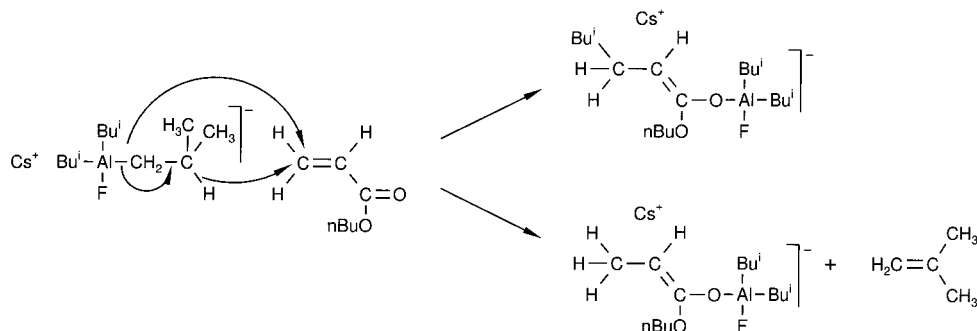


Figure 9. Determination of the reaction order with respect to the concentration of the complex $[\text{Cs}[\text{Al}_2\text{Bu}_6\text{F}]]$ for the anionic polymerization of n BuA with $\text{EiBLi/Cs}[\text{Al}_2\text{Bu}_6\text{F}]$ in toluene at -78°C described in Figure 8. Initial apparent rate constant (■), slope 1.1 ± 0.1 ; final apparent rate constant (▲), slope 0.9 ± 0.1 .

cussed.^{3,4} Furthermore, NMR and quantum-chemical calculations show that the interactions between aluminum alkyls, ester enolates, and ester groups of monomer and polymer are very complex.^{5,11} An ester enolate-aluminum alkyl complex might be responsible for the slow reaction at the beginning. In the presence of a high concentration of the complex we suppose the formation of a more reactive species; different associates may exist for each active species.³ Moreover, it cannot be excluded that the position of the equilibria and the degree of association of the living chain ends depend on their degree of polymerization. It has been shown previously that low molecular weight ester enolates differ in their behavior compared to the corresponding polymer chain ends. They deviate in their degree of aggregation^{12,13} and their reactivity.¹⁴⁻¹⁶ As the molecular weight distributions of the polymers obtained at the beginning of the reaction are broad, the establishment of the equilibrium of active species and/or associates during the polymerization should be slow with respect to propagation.¹⁷

Surprisingly, the initiator efficiency increases up to values of $f \approx 3$ with increasing complex concentration (cf. Table 2). Transfer reactions can be excluded from the linearity of the plots of the number-average degree of polymerization vs monomer conversion (see Figure 6). A possible explanation could be that the complex itself acts as an initiator. Thus, we performed a polymerization at high complex concentration in the absence of the initiator EiBLi . After 4 h, 80% conversion was reached, yielding a polymer with $M_n = 53\,700$ and a broad molecular weight distribution ($M_w/M_n = 1.8$). A MALDI-TOF mass spectrum shows two homologous series with residual masses of 41 and 97 Da (Figure 10), which are supposed to result from initiation with

Scheme 1. Proposed Equilibrium between Ester Enolate/ AlR_3 and Ester Enolate/ $\text{Cs}[\text{AlR}_3\text{F}]$ Complexes ($m, n = 1-4$)**Scheme 2. β -Hydride Transfer and Initiation of $n\text{BuA}$ with the Complex $\text{Cs}[\text{Al}_2\text{Bu}'_6\text{F}]$** **Table 3. Temperature Dependence of the Anionic Polymerization of $n\text{BuA}$ with $\text{EtBLi}/\text{Cs}[\text{Al}_2\text{Bu}'_6\text{F}]$ in Toluene^a**

$T/^\circ\text{C}$	$k_{\text{app}}/10^{-4} \text{ s}^{-1}$	$K_{\text{app}}/10^{-4}$	$k_t/10^{-3} \text{ s}^{-1}$	k_{app}/k_t	x_p	M_n	M_w/M_n	f	$[\text{P}^*]_0/10^{-4} \text{ mol L}^{-1}$	$k_p/\text{mol L}^{-1} \text{ s}^{-1}$	$K_p'/\text{mol L}^{-1} \text{ s}^{-1}$
-78	1.5	25.9			1.00	47 000	1.09	1.28	6.3	0.24	4.1
-65	13.8	58.2			1.00	46 000	1.07	1.29	6.3	2.19	9.2
-50	31.3		1.4	2.2	0.89	59 300	1.5	0.95	4.7	6.66	
-40	45.1		6.3	0.7	0.53	35 300	1.8	0.96	4.7	9.60	

^a $[\text{EtBLi}]_0 = 4.9 \times 10^{-4} \text{ mol/L}$, $[n\text{BuA}]_0 = 0.234 \text{ mol/L}$, $[\text{AlBu}'_3]/[\text{CsF}] = 3.5/1.7 \times 10^{-3} \text{ mol/L}$.

hydride and with an isobutyl anion, respectively (Scheme 2). In contrast, the MALDI-TOF mass spectra of a polymer sample initiated by EtBLi shows only polymer chains with EtB (residual mass 155 Da) and hydride end groups (Figure 11).

Temperature Dependence. An upward curvature is found in the time-conversion plots below -65°C (Figure 12), and the molecular weight distributions of the polymers obtained are narrow ($M_w/M_n < 1.1$, see Table 3). However, the reaction loses its living character at higher temperatures. At -50°C the time-conversion plot is curved downward, indicating the occurrence of termination reactions. GPC analysis shows a UV absorption at $\lambda = 260 \text{ nm}$ which is characteristic for enolized cyclic β -ketoester end groups.¹⁰ Consequently, the molecular weight distribution broadens ($M_w/M_n > 1.5$). The Arrhenius plot of the propagation rate constants obtained from the initial slopes is linear in the observed temperature range (Figure 13); the apparent values of the activation parameters are $E_a^{\text{app}} = 29.8 \pm 3.1 \text{ kJ/mol}$ and $\log A_{\text{app}} = 7.7 \pm 0.8$. The calculated activation energy is higher than those usually obtained with various counterions and solvents. In toluene, values between 17 and 23 kJ/mol were reported for $\text{Li}^+/\text{AlMe}_3/\text{MPiv}$,⁶ $\text{Li}^+/\text{lithium 2-ethoxyethoxide}$,¹⁸ and GTP.¹⁹ Only the activation energy of the polymerization in the presence of tetramethylammonium chloride-triisobutylaluminum is comparable to this value.⁶ Since the k_p values depend on the complex concentration, it becomes clear that they are apparent ones, being related to the equilibrium constants of the equilibria involved. Consequently, the apparent activation parameters contain the entropies and enthalpies of these equilibria.

Homo- and Copolymerization of Different Acrylates. Apart from the polymerization of $n\text{BuA}$, those of

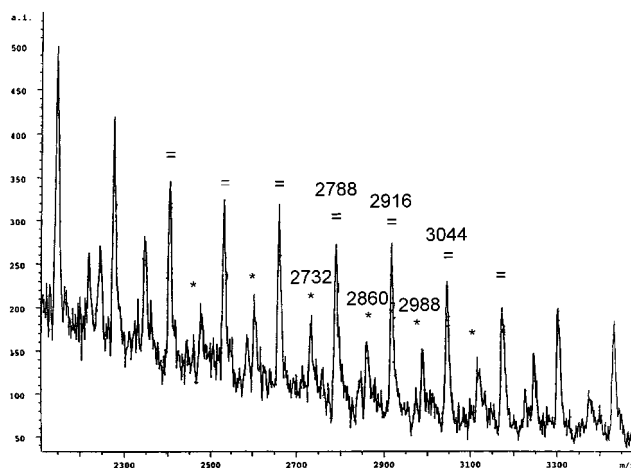


Figure 10. MALDI-TOF mass spectrum of a PnBuA obtained with $\text{Cs}[\text{Al}_2\text{Bu}'_6\text{F}]$ in toluene at -78°C . $[n\text{BuA}]_0 = 0.234 \text{ mol/L}$, $[\text{AlBu}'_3]/[\text{CsF}] = 14.0/7.2 \times 10^{-3} \text{ mol/L}$. The masses correspond to potassium adducts $[\text{M}-\text{K}^+]$. Repeat unit of all series: 128.2 Da, (*) H^- -initiated (residual mass, 41 Da = $m(\text{H}) + m(\text{H}) + m(\text{K}^+)$); (=) Bu' -initiated (residual mass, 97 Da = $m(\text{Bu}') + m(\text{H}) + m(\text{K}^+)$).

2-ethylhexyl acrylate (EHA), allyl acrylate (AlA), and dihydrocyclopentadienyl acrylate (DCPA) are also living and controlled in the presence of $\text{Cs}[\text{Al}_2\text{Bu}'_6\text{F}]$ in toluene at -78°C . In all cases, linear plots of the number-average degree of polymerization vs the monomer conversion and polymers with high molecular weights and narrow molecular weight distributions (see Figure 14) are obtained ($M_w/M_n < 1.2$). The controlled random copolymerization of EHA and DCPA is achieved with the same complex under identical reaction conditions (Figure 14), leading to polyacrylates with pendant

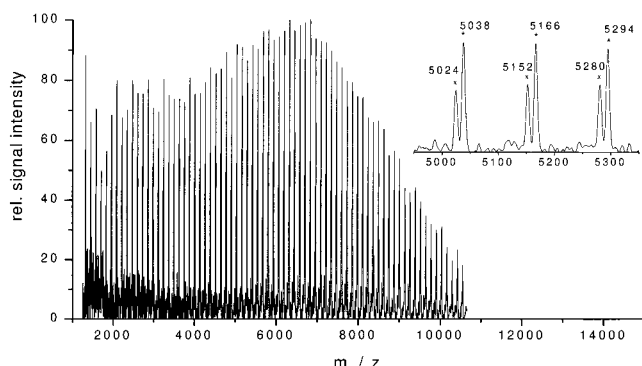


Figure 11. MALDI-TOF mass spectrum of a PnBuA obtained with $\text{EiBLi/Cs[Al}_2\text{Bu}_6\text{F]}$ in toluene at -78°C . $[\text{EiBLi}]_0 = 4.9 \times 10^{-4} \text{ mol/L}$, $[\text{BuA}]_0 = 0.234 \text{ mol/L}$, $[\text{AlBu}_3]/[\text{CsF}] = 14.0/7.2 \times 10^{-3} \text{ mol/L}$. The masses correspond to potassium adducts $[\text{M-K}^+]$. Repeat unit of all series: 128.2 Da , (*) H^- -initiated (residual mass, $41 \text{ Da} = m(\text{H}) + m(\text{H}) + m(\text{K}^+)$); (x) EiB^- -initiated (residual mass, $155 \text{ Da} = m(\text{EiB}) + m(\text{H}) + m(\text{K}^+)$).

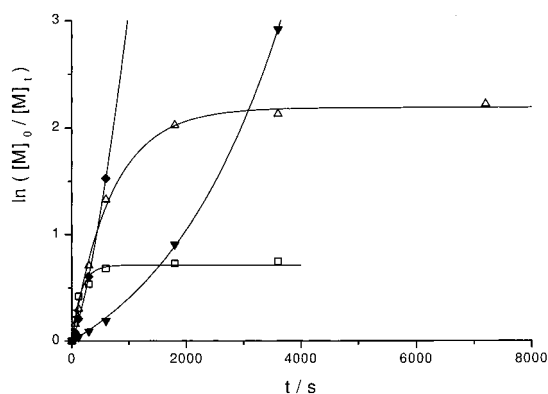


Figure 12. First-order time-conversion plots for the anionic polymerization of BuA with $\text{EiBLi/Cs[Al}_2\text{Bu}_6\text{F]}$ in toluene at -78°C (\blacktriangle), -65°C (\blacklozenge), -50°C (\triangle), and -40°C (\square). For reaction conditions see Table 3.

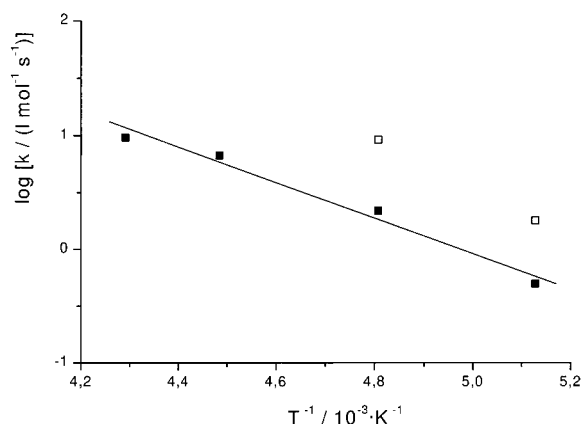


Figure 13. Arrhenius plot for the anionic polymerization of BuA with $\text{EiBLi/Cs[Al}_2\text{Bu}_6\text{F]}$ in toluene; for reaction conditions see Figure 12. Initial apparent rate constant k_p : $E_a = 29.8 \pm 3.1 \text{ kJ/mol}$, $\log A = 7.7 \pm 0.8$ (\blacksquare). Final apparent rate constant k_p' (\square).

unsaturated groups which can be used for further cross-linking reactions.

Synthesis of Graft Copolymers. The random copolymerization of BuA with acryloyl-functionalized PMMA macromonomers leads to graft copolymers PnBuA-*g*-PMMA. Usually, it is difficult to obtain these polymers by anionic copolymerization, because the macromonomers cannot be purified sufficiently—due to the presence of the aluminum alkyl, this polymerization

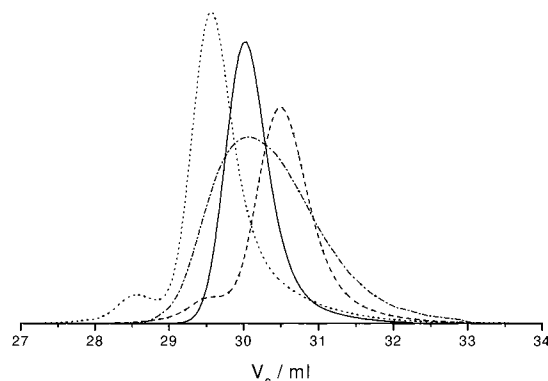


Figure 14. GPC eluograms of polyacrylates obtained in the anionic polymerization at -78°C with $\text{EiBLi/Cs[Al}_2\text{Bu}_6\text{F]}$ in toluene. $[\text{EiBLi}]_0 = 4.9 \times 10^{-4} \text{ mol/L}$, $[\text{M}]_0 = 0.23 \text{ mol/L}$, $[\text{AlBu}_3]/[\text{CsF}] = 3.5/1.7 \times 10^{-3} \text{ mol/L}$, PEHA (—, $M_n = 63\,400$, $M_w/M_n = 1.05$, $x_p = 0.63$); PDCPA (---, $M_{n,\text{app}} = 48\,900$, $M_w/M_n = 1.11$, $x_p = 0.64$); PAIA (- · -, $M_{n,\text{app}} = 51\,200$, $M_w/M_n = 1.19$, $x_p = 0.96$); poly(EHA-*co*-DPCA): $[\text{EHA}]_0 = 0.202 \text{ mol/L}$, $[\text{DPCA}]_0 = 0.024 \text{ mol/L}$, (\cdots , $M_{n,\text{app}} = 76\,500$, $M_w/M_n = 1.14$, $x_p = 1$).

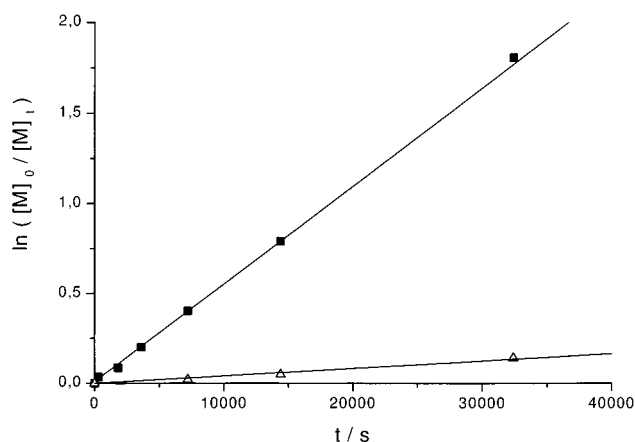


Figure 15. First-order time-conversion plots for the anionic copolymerization of BuA and PMMA-macromonomer (MM) with $\text{EiBLi/Cs[Al}_2\text{Bu}_6\text{F]}$ in toluene at -78°C ; BuA (\blacksquare), PMMA-MM (\triangle). $[\text{EiBLi}]_0 = 1.2 \times 10^{-3} \text{ mol/L}$, $[\text{BuA}]_0 = 0.146 \text{ mol/L}$, $[\text{MM}]_0 = 2.6 \times 10^{-3} \text{ mol/L}$, $[\text{AlBu}_3]/[\text{CsF}] = 4.5/2.2 \times 10^{-3} \text{ mol/L}$.

is self-cleaning here. The time-conversion plot (Figure 15) shows quantitative conversion of BuA but incomplete macromonomer conversion (only 28%).

By using the Jaacks method,²⁰ a very high reactivity ratio of BuA ($r_1 = 9.8$, see Figure 16) is observed, even higher than that in the anionic copolymerization of styrene with polystyrene macromonomers ($r_1 = 2.0$)²¹ or MMA with PMMA macromonomers ($r_1 = 1.9$).²² The extremely low reactivity of the macromonomer as compared to the low molecular weight comonomer leads to incomplete conversion. This might be explained by the incompatibility of backbone and side chains in the reaction solution, which causes the deviation from ideal copolymerization, also indicated by the nonlinearity of the Jaacks plot. Nevertheless, the molecular weight distribution of the observed graft copolymer is narrow ($M_w/M_n = 1.3$, see Figure 17).

Conclusions

The polymerization of meth(acrylates) initiated by EiBLi in the presence of the $\text{Cs[Al}_n\text{R}_{2n}\text{X}]$ ($n = 1, 2$; $\text{R} = \text{Et, Bu}$) has a living and controlled character only for selected combinations of the complex, so that the

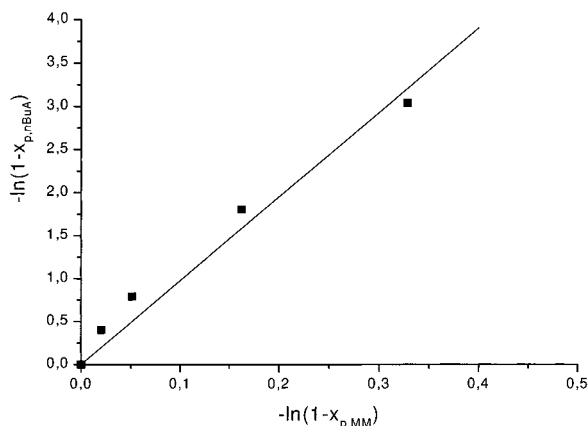


Figure 16. Determination of the reactivity ratio of n BuA in the copolymerization with PMMA—macromonomer using the Jaacks method,²⁰ $r_1 = 9.8 \pm 0.6$.

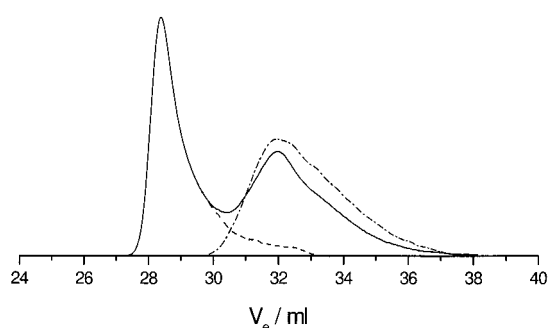


Figure 17. GPC eluogram of a graft copolymer PnBuA-*g*-PMMA obtained from the anionic copolymerization of n BuA and an acryloyl-functionalized PMMA macromonomer at -78°C with $\text{EtBLi}/\text{Cs}[\text{Al}_2\text{Bu}_6\text{F}]$ in toluene. Crude product (—); graft copolymer (---), $M_{n,\text{app}} = 86\,000$, $M_w/M_n = 1.3$; PMMA macromonomer (- · -), $M_n = 7100$, $M_w/M_n = 1.8$. n BuA/MM = 1/1 w/w; conversions: n BuA: 0.96, MM: 0.28.

reaction conditions for each monomer have to be optimized. The reaction follows first-order kinetics with respect to the initial concentration of initiator, monomer, and complex. The curved time–conversion plots as well as the bimodal molecular weight distributions of the polymers sometimes obtained at low conversion, getting unimodal and narrow at higher monomer conversion, indicate equilibria between at least two active species of different reactivity. Further investigations of

the structures of the active species, e.g., NMR measurements, are necessary to prove the proposed mechanism. The successful homo-, random, and block copolymerization of several (meth)acrylates and the synthesis of graft copolymers show the versatility of this new initiating system.

Acknowledgment. We thank Dr. Helmut Schlaad (Potsdam) for helpful suggestions and Mrs. Nicole Gilbert and Mr. Peter Blumers for their very helping hands. This work was supported by the German Bundesministerium für Bildung, Wissenschaft, Forschung und Technologie (Project No. 03N 3006 A5 and 03N 30043), by BASF AG, Ludwigshafen, Germany, and by the Deutsche Forschungsgemeinschaft (Grant Mu 896/9-1).

References and Notes

- (1) Schlaad, H.; Schmitt, B.; Müller, A. H. E. *Angew. Chem.* **1998**, *110*, 1497; *Angew. Chem., Int. Ed. Engl.* **1998**, *37*, 1389.
- (2) Schlaad, H.; Schmitt, B.; Müller, A. H. E.; Jüngling, S.; Weiss, H. *Macromol. Symp.* **1998**, *132*, 293.
- (3) Schlaad, H.; Müller, A. H. E. *Macromolecules* **1998**, *31*, 7127.
- (4) Schmitt, B.; Müller, A. H. E. *Macromolecules*, in press.
- (5) Schmitt, B.; Schlaad, H.; Müller, A. H. E.; Mathiasch, B.; Steiger, S.; Weiss, H. *Macromolecules* **2000**, *33*, 2887.
- (6) Schmitt, B. Dissertation, Universität Mainz, 1999.
- (7) Fieberg, A.; Broska, D.; Heibel, C.; Bandermann, F. *Des. Monomers Polym.* **1998**, *1*, 285.
- (8) Ziegler, K.; Köster, R.; Lehmkühl, H.; Reinert, K. *Liebigs Ann. Chem.* **1960**, *629*, 33.
- (9) Lochmann, L.; Lim, D. *J. Organomet. Chem.* **1973**, *50*, 9.
- (10) Janata, M.; Lochmann, L.; Müller, A. H. E. *Makromol. Chem.* **1990**, *191*, 2253.
- (11) Schmitt, B.; Schlaad, H.; Müller, A. H. E.; Mathiasch, B.; Steiger, S.; Weiss, H. *Macromolecules* **1999**, *32*, 8340.
- (12) Halaska, V.; Lochmann, L. *Collect. Czech. Chem. Commun.* **1973**, *38*, 1780.
- (13) Kunkel, D.; Müller, A. H. E.; Lochmann, L.; Janata, M. *Makromol. Chem., Macromol. Symp.* **1992**, *60*, 315.
- (14) Tsvetanov, C. B.; Müller, A. H. E.; Schulz, G. V. *Macromolecules* **1985**, *18*, 863.
- (15) Müller, A. H. E.; Lochmann, L.; Trekoval, J. *Makromol. Chem.* **1986**, *187*, 1473.
- (16) Baskaran, D.; Müller, A. H. E. *Macromolecules* **1997**, *30*, 1869.
- (17) Litvinenko, G.; Müller, A. H. E. *Macromolecules* **1997**, *30*, 1253.
- (18) Maurer, A. Dissertation, Universität Mainz, 1998.
- (19) Zhuang, R.; Müller, A. H. E. *Macromolecules* **1995**, *28*, 8043.
- (20) Jaacks, V. *Makromol. Chem.* **1972**, *161*, 161.
- (21) Gnanou, Y.; Lutz, P. *Makromol. Chem.* **1989**, *190*, 577.
- (22) Schlaad, H. Dissertation, Universität Mainz, 1997.

MA9916640